Cooling the Tip of a Turbine Blade Using Pressure Side Holes—Part I: Adiabatic Effectiveness Measurements

J. R. Christophel

K. A. Thole

Mechanical Engineering Department,
Virginia Polytechnic Institute and State University,
Blacksburg, Virginia 24061

F. J. Cunha

Pratt & Whitney,
United Technologies Corporation,
East Hartford, Connecticut 06108

Durability of turbine blade tips has been and continues to be challenging, particularly since increasing turbine inlet temperatures is the driver for improving turbine engine performance. As a result, cooling methods along the blade tip are crucial. Film-cooling is one typically used cooling method whereby coolant is supplied through holes placed along the pressure side of a blade. The subject of this paper is to evaluate the adiabatic effectiveness levels that occur on the blade tip through blowing coolant from holes placed near the tip of a blade along the pressure side. A range of blowing ratios was studied whereby coolant was injected from holes placed along the pressure side tip of a large-scale blade model. Also present were dirt purge holes on the blade tip, which is part of a commonly used blade design to expel any large particles present in the coolant stream. Experiments were conducted in a linear cascade with a scaled-up turbine blade whereby the Reynolds number of the engine was matched. This paper, which is Part 1 of a two part series, compares adiabatic effectiveness levels measured along a blade tip, while Part 2 combines measured heat transfer coefficients with the adiabatic effectiveness levels to assess the overall cooling benefit of pressure side blowing near a blade tip. The results show much better cooling can be achieved for a small tip gap compared with a large tip gap with different flow phenomena occurring for each tip gap setting.
[DOI: 10.1115/1.1812320]

Introduction

The performance of a turbine engine is a strong function of the maximum gas temperature at the rotor inlet. Because turbine airfoils are exposed to hot gas exiting the combustion chambers, the materials and cooling methods are of critical importance. Turbine blade designers concentrate heavily on finding better cooling schemes to increase the overall operational life of all turbine airfoils, namely the high pressure turbine blades. The clearance between the blade tip and the associated shroud, also known as the blade outer air seal, provides a flow path across the tip that leads to aerodynamic losses and high heat transfer rates along the blade tip. The flow within this clearance gap is driven by a pressure differential between the pressure and suction side of the blade, but is also affected by the viscous forces as the fluid comes into contact with the walls of the gap.

The goal of the work presented in this paper is to assess a cooling hole arrangement whereby holes are placed near the tip of a blade along the pressure side. Note that holes are also located on the tip, which are dirt purge holes that are required to expel dirt from the coolant stream. Comparisons of performance were made for a range of coolant flows at two different tip gap settings. The comparisons made in this paper (Part I) have been made through measurements of the adiabatic effectiveness along the turbine blade tip. A companion paper, Part II [1], provides a full heat transfer analysis including the overall benefit of film-cooling on the tip.

Contributed by the International Gas Turbine Institute (IGTI) of THE AMERICAN SOCIETY OF MECHANICAL ENGINEERS for publication in the ASME JOURNAL OF TURBOMACHINERY. Paper presented at the International Gas Turbine and Aeroengine Congress and Exhibition, Vienna, Austria, June 13–17, 2004, Paper No. 2004-GT-53251. Manuscript received by IGTI, October 1, 2003; final revision, March 1, 2004. IGTI Review Chair: A. J. Strazisar.

Relevant Past Studies

One method for improving the thermal environment along the blade tip is to inject coolant into the tip region. In a review paper on tip heat transfer, Bunker [2] states that for a blade tip there has been very little film-cooling research reported in the literature even though film-cooling is widely used. Blowing from the tip has been considered by Kim and Metzger [3], Kim et al. [4], Kwak and Han [5,6], Acharya et al. [7] and Hohlfeld et al. [8].

Kim et al. [4] present a summary of the experimental work that D. Metzger performed on tip blowing. In addition to concluding that there is only a weak effect of the relative motion between a simulated blade and shroud on tip heat transfer coefficient, they stated that there is a strong dependency of adiabatic effectiveness on the shape of the hole and injection locations. Note that a more recent study by Srinivasan and Goldstein [9], who used an actual airfoil, also indicated a negligible effect of the relative motion between the tip and shroud on tip heat transfer coefficients with the exception being near the leading edge region. Four hole configurations were discussed by Kim et al. [4] that included the following: discrete slots located along the blade tip, round holes located along the blade tip, angled slots positioned along the pressure side, and round holes located within the cavity of a squealer tip. The studies reported by Kim et al. were performed in a channel that simulated a tip gap, whereby no blade with its associated flow field was simulated. In comparing the discrete slots to the holes, their data indicated a substantial increase in adiabatic effectiveness using the discrete slots for all blowing ratios tested. Injection from the pressure side holes provided cooling levels of similar magnitude to the holes placed on the tip. Kim et al. also reported that an increase in coolant mass flow for the discrete slots and pressure side flared holes generally yielded improved cooling to a given mass flux ratio beyond which increased coolant yielded decreased cooling effectiveness.

Kwak and Han [5,6] reported measurements for varying tip gaps with cooling holes placed along the pressure surface at a 30°

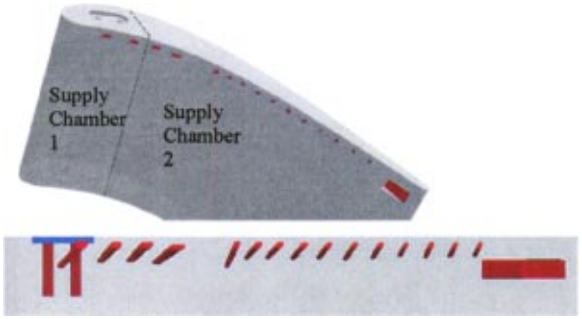

Fig. 1 Schematic showing the approximate hole placement for the tip model

breakout angle and on the tip surface at a 90 deg angle for a flat and a squealer tip geometry. They found a substantial improvement in effectiveness with the addition of a squealer tip. The coolant circulated within the squealer tip providing a better distribution of the coolant along much of the tip compared with no squealer cases. Only along parts of the suction side was the adiabatic effectiveness poor. They found that for the flat tip, good cooling was provided to the trailing edge resulting from the accumulation of coolant that exited in this area. Their results also indicated that more coolant resulted in improved effectiveness.

One of the recent computational studies by Ameri [10] indicated that a sharp edge along the pressure side (with no blowing) was more effective in reducing the tip leakage flow relative to an rounded edge. Predictions for varying tip gap sizes by Acharya et al. [8] indicated that film-cooling injection lowered the local pressure ratio and altered the nature of the leakage vortex. High film-adiabatic effectiveness and low heat transfer coefficients were predicted along the coolant trajectory with the lateral spreading of the coolant jets being quite small for all cases. With an increased tip gap the coolant was able to provide better downstream effectiveness through increased mixing. For the smallest tip gap, the coolant was shown to impinge directly on the surface of the shroud leading to high film effectiveness at the impingement point. As the gap size increased, their predictions indicated that the coolant jets were unable to penetrate to the shroud. Computational results by Hohlfeld et al. [8] indicated that as the blowing ratio is increased for a large tip gap, the tip cooling increased only slightly while the cooling to the shroud increased significantly.

In summary, there are only a limited number of studies that have addressed blowing in the tip gap region. None of these studies compared effectiveness levels for different blowing ratios from cooling holes placed along the pressure side of an actual blade geometry.

Description of Cooling Hole Configuration

Figure 1 is a schematic showing the approximate cooling hole placement along the pressure side of the turbine blade. For proprietary reasons the exact hole locations and orientations are not given. This geometry had a dirt purge cavity that was recessed two small gap heights ($2h$) and 0.67 large gap heights ($0.67H$) from the tip surface. Within this cavity were two dirt purge holes, which have been described in detail by Hohlfeld et al. [8]. In addition to the dirt purge holes, the tip geometry had 15 pressure side holes placed close to the tip surface. The four film-cooling holes just downstream of the stagnation were slightly expanded in the axial direction and had a metering hole diameter of $0.56D$, where D is the diameter of the dirt purge holes, and the remainder of the holes had no expansion with a metering hole diameter of $0.4D$. There was also a slot at the trailing edge called the trailing edge flag (TEF). Table 1 further summarizes the hole geometry in this study.

Table 1 Description of hole model

Parameter	
No. of cooling holes	15
Coolant flow area (dirt purge, cooling holes, andTEF) (cm^2)	5.15
Hole metering area/Coolant flow area	0.51
Dirt purge flow area/Coolant flow area	0.33
TEF flow area/Coolant flow area	0.16

To ensure good control on the blowing ratios through the holes, which will be further discussed in the next section, a dividing wall was placed within the blade cavity to allow for two different supplies inside the blade. The tip model had the separating wall placed after the second cooling hole downstream of the stagnation location. These two different supply cavities are also illustrated in Fig. 1. Each cavity was supplied by a separate coolant flow source such that independent control of the coolant flow rates could be achieved. The placement of the supply cavities was based on best matching to the local blowing ratios of the engine.

Outlines of the holes were made from stereo lithography (SLA) to allow for a good replication of the hole geometry. Because the SLA material does not have a sufficiently low thermal conductivity, the models were designed to have foam molded around the holes and supply chambers. After the SLA model of the hole outlines were made, the SLA model was placed inside a mold of the blade geometry. A polyurethane foam compound, with a thermal conductivity of 0.04 W/m^2 K, was poured in the blade mold and then allowed to expand and harden. The combined SLA holes and foam blade were then removed from the mold, attached as the tip to an SLA blade, and then placed in the wind tunnel for testing. The molded tip model extended 28% of the blade span. Pictures of the combined SLA hole model and foam blade for the holes are shown in Fig. 2.

Experimental Facilities

The experimental facility for this work consisted of a large-scale, low-speed, closed-loop wind tunnel providing an inlet velocity to the test section of 12 m/s to match engine Reynolds number conditions for a 12× blade model. The blade geometry and flow conditions are summarized in Table 2 with a diagram of the wind tunnel and test section shown in Figs. 3(*a*) and 3(*b*). Starting at the fan, flow passed through a primary heat exchanger to obtain a uniform temperature profile before being divided into three passages. The main passage, located in the center, has a heater that was used to achieve hot mainstream gas, while flow to the two auxiliary passages was used to supply a single row of high momentum jets used to generate a high turbulence level to the cascade. The inlet turbulence level, measured one chord upstream, was 10% and the length scale was 11 cm. Flow entered the test section, consisting of the blade model as shown in Fig. 3(*b*). An independent compressed air supply provided the coolant flow to the two cavities, which was ultimately injected through cooling holes placed in the blade tip.

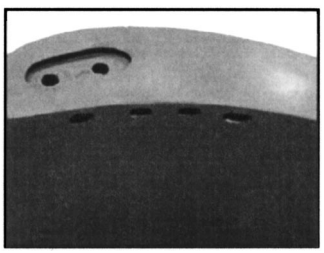

Fig. 2 Photo of SLA/foam model for the dirt purge and cooling holes

Table 2 Blade geometry and flow conditions

Parameter	Wind tunnel settings
Scaling factor	12×
Axial chord/True chord	0.66
Pitch/True chord	0.81
Span/True chord	1.03
Re_{in}	2.1×10^5
Inlet Angle, θ	16.5 deg
Coolant to Mainstream ΔT (°C)	25
Small tip gap/Span (%)	0.54
Large tip gap/Span (%)	1.63

The blade test section consisted of a two passage linear cascade as shown in Fig. 3(*b*). Velocity measurements were taken approximately one chord upstream at a number of pitch-wise locations to verify a uniform incoming velocity field. Static pressure taps were located near the mid-span of the central blade to compare the pressure distribution around the blade to that of an inviscid CFD prediction with periodic boundary conditions. Matching the pressure distribution around the blade ensured equal flow distribution between each of the respective flow passages, and ensured the correct driving pressures across the tip gap. The nondimensional pressure distributions for the central blade are shown in Fig. 4 for representative large and small tip gap settings. Also shown on this graph is the placement of the supply chambers separating the front and back set of holes as well as the stagnation location ($S/S_{max}=0$). Negative values of S/S_{max} are on the pressure side.

Because coolant was supplied to two independently controlled plenums, which also included the supplies for the dirt purge holes and TEF, a number of experiments were conducted to deduce a discharge coefficient for each cooling component to ensure correct cooling flows were ultimately set. The tip had four cooling components: (i) front plenum film-cooling holes, (ii) dirt purge holes, (iii) back plenum film-cooling holes, and (iv) TEF. The discharge coefficients were found by isolating each component while the other three components were sealed. By measuring the supply chamber pressure, the calculated flow rate could be compared to that of the measured flow rate using a venturi flow meter.

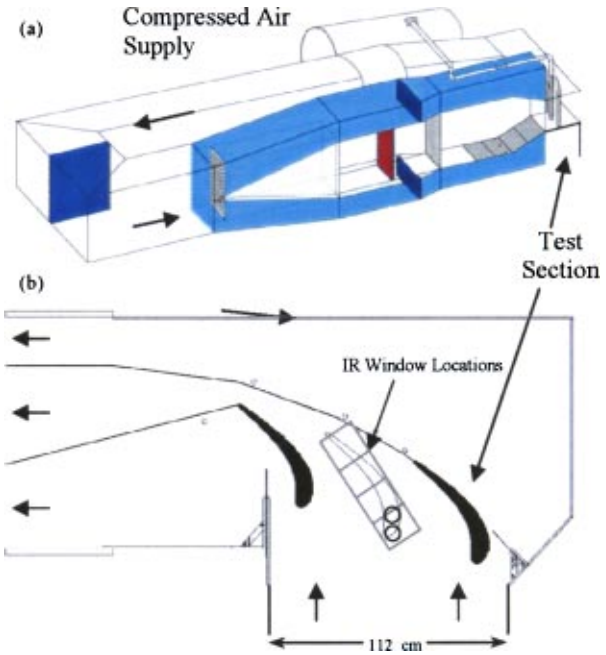

Fig. 3 Schematic of (*a*) wind tunnel facility and (*b*) test section for the blade tips

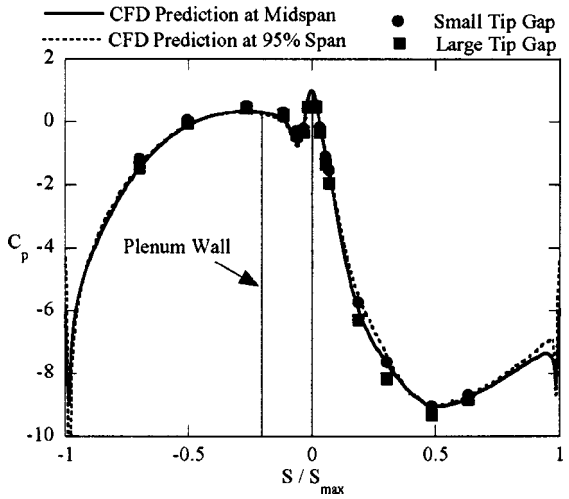

Fig. 4 Predicted and measured static pressure distributions for the large and small tip gap cases

The measured discharge coefficients for the cooling holes are shown in Fig. 5. The front and back holes of the tip model approached nominally the same value ($C_d=0.64$), which is expected because the hole geometries were very similar. As a check on the accuracy of using the previously described method for setting the coolant flows, a comparison was made between the total coolant flow to the entire tip measured using the venturi flow meter and that calculated using the measured pressures combined with the discharge coefficients. The coolant mass balance was within 2.8% for all experimental cases.

Several parameters were considered when comparing the low speed wind tunnel tests to that of an actual engine. A matrix of tests was designed to assess the effects of the blowing ratio, momentum flux ratio, and tip gap setting. The flow split for each of the cases is given in Table 3. For the blowing ratios given for the holes, local values of the external velocity and mass flux through the hole were used. To compute the local external velocity at each hole exit, the predicted static pressure at the 95% span location of the blade (also shown on Fig. 4) was used at each hole location. The coolant velocity through the holes was based on the velocity at the metering area of the hole. The local blowing ratios that were tested are shown in Fig. 6. The density ratio of the jet to mainstream used during testing was 1.08.

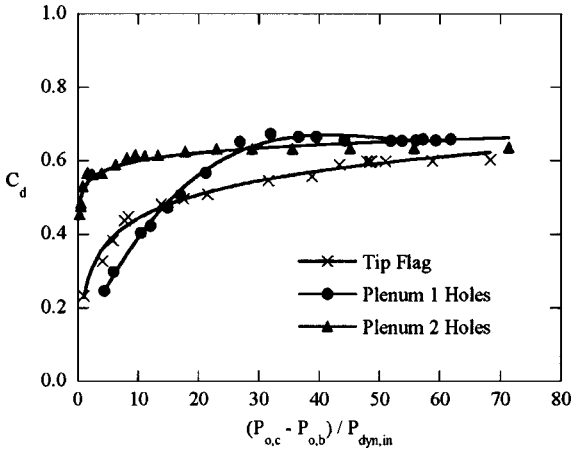

Fig. 5 Discharge coefficients that were measured for the cooling holes, dirt purge holes, and TEF

Table 3 Matrix of experiments

Gap. setting	Total coolant flow (% passage)	Flow split plenums 1/2 (% coolant)
Small, Large	0.47	58/42
Small, Large	0.58	59/41
Small, Large	0.68	59/41
Small, Large	1.0	51/49
Small no dirt purge flow	0.07	100/0

The four nominal total coolant flow rates were 0.47%, 0.58%, 0.68%, and 1.0%. These percentages are given relative to the mainstream passage flow through the blades. In Fig. 6, the blowing ratios are shown for the small tip gap. There was no difference in the blowing ratios with gap height. Figure 7 provides the percentage difference between the CFD predicted and measured distribution of coolant for the 0.68% cooling flow case through each of the film holes, the dirt purge holes, and TEF. Note that the 0.68% refers to the total coolant flow relative to the total blade passage flow. There was good agreement between the individual flow rates for each hole as predicted by CFD and calculated experimentally using the discharge coefficients and measured pressures. The comparisons indicated that the largest difference was 0.45%, which occurred for the fourth cooling hole.

Experimental Methodology. Investigation of the hole geometries required obtaining surface temperatures on the foam model, representing the adiabatic surface temperatures along the tip. Typical operating conditions consisted of a temperature differential between the coolant flow and hot mainstream by approximately 25°C. The mainstream and coolant supply chamber temperatures were measured during the experiments with type E thermocouples. The coolant temperatures were measured inside the two plenums. Each test required the wind tunnel and tip models to reach a thermal equilibrium, which required approximately 4 h. Temperatures and flows were monitored during this time to ensure equilibrium conditions. The tip gaps were set by raising or lowering the blade using a threaded rod to the gap setting. This technique required the use of a precisely machined plate placed under the tip to ensure the correct gap.

The tip surface temperatures were obtained using an Inframetrics P20 infrared (IR) camera. The images were processed with Thermacam Researcher 2002® and an in-house MATLAB code. As shown by the boxes in Fig. 3(*b*), four IR images were acquired

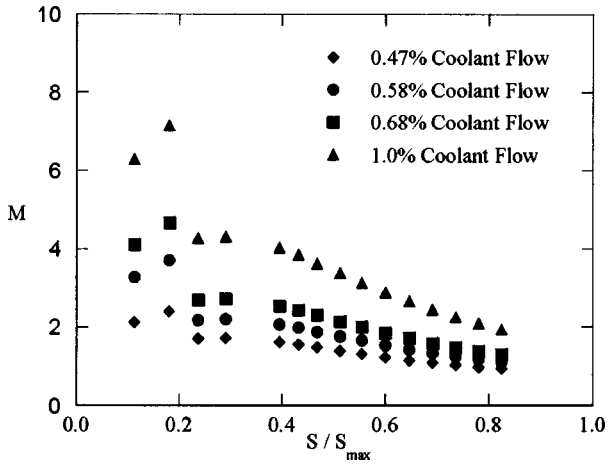

Fig. 6 Local mass flux ratios for each of cooling holes placed on the pressure side of the blade

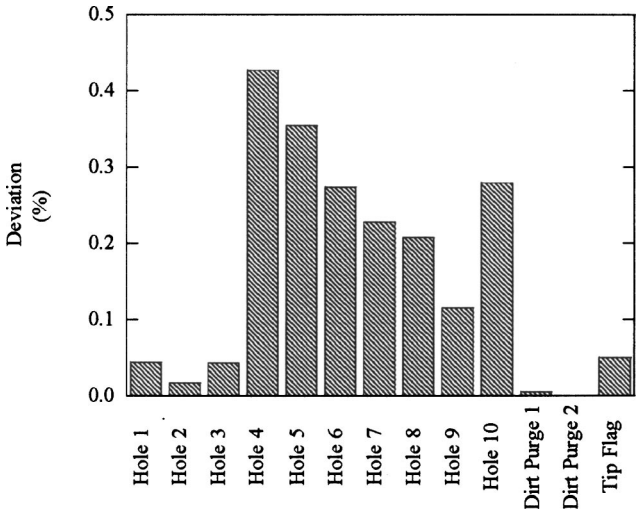

Fig. 7 Percent difference between computational and experimental flow rates at 0.68% coolant flow

through the zinc selenide windows placed in the shroud surface to cover the entire blade, which transmitted the radiation. Each image covered an area that was 21.3 cm by 16 cm and contained 320 by 240 pixels. The camera was located approximately 55 cm from the tip and resulted in a spatial resolution of 0.63 mm. For every test, each of the four images was taken five times and the averaged radiation values were used.

The calibration process for the camera required direct comparisons of measured surface temperatures, using thermocouple strips placed on the tip surface, with the infrared radiation collected by the camera. Thermocouple strips were used to ensure accurate surface temperatures were measured. These strips were placed on the blade tip using a thermally conducting bonding agent. After the experiments were completed, the infrared image was processed whereby the emissivity and background temperature of the infrared pixels nearby the surface thermocouple were adjusted to ensure agreement between the measured temperatures. Each of the four images was processed in a similar manner whereby six thermocouples were ultimately used to ensure all four images were accurately calibrated. An emissivity of 0.83 was used for all the images while the background temperatures were adjusted to ensure a calibrated image. This process resulted in an agreement between all of the thermocouples and infrared temperatures to within 1.0°C, thereby giving a difference in effectiveness of η of ± 0.04.

Overall uncertainties were calculated for nondimensional adiabatic effectiveness levels (η) according to the partial derivative method described in Moffat [11]. The total uncertainty of all measurements was calculated as the root of the sum of the squares of the precision uncertainty and the bias uncertainty. The precision uncertainty for measurements made with the infrared camera was determined through an analysis of five calibrated images taken in succession on one portion of the tip at constant conditions. The precision uncertainty was calculated to be 0.31°C, which is the standard deviation of the five readings based on a 95% confidence interval. The camera manufacturer reported the bias uncertainty as 2.0% of the full scale. The largest scale used in this study was 20°C though some images could be captured on a 10°C range. The thermocouples measuring the free-stream and coolant temperatures were reported by the manufacturer to read within ±0.2°C. The total uncertainty in effectiveness was found to be $\partial\eta = \pm 0.046$ at $\eta = 1$ and $\partial\eta = \pm 0.046$ at $\eta = 0.2$.

Computational Methodology. To better understand the effects of these hole shapes, computational fluid dynamics (CFD) simulations were also performed. A commercially available CFD

code, Fluent 6.0 [12], was used to perform all simulations. Fluent is a pressure-based flow solver that can be used with structured or unstructured grids. An unstructured grid was used for the study presented in this paper. Solutions were obtained by numerically solving the Navier–Stokes and energy equation through a control volume technique. All geometric construction and meshing were performed with GAMBIT. To ensure a high quality mesh, the flow passage was divided into multiple volumes, which allowed for more control during meshing. The tip gap region was of primary concern and was composed entirely of hexahedral cells with an aspect ratio smaller than three.

Computations were performed on a single turbine blade exposed to periodic conditions along all boundaries in the pitch direction. Inlet conditions to the model were set as a uniform inlet velocity at approximately one chord upstream of the blade. An inlet mass flow boundary condition was imposed for the coolant at the plenum entrance for the cooling holes. The mesh contained approximately 20 grid points across the hole exit. Mainstream flow angles were set to those of the experiments as well as the scaled values for the engine while the turbulence levels and mixing length were set to 1% and 0.1 m, respectively. Computations were also performed with an inlet turbulence level of 10%, but no noticeable differences were predicted between the 1% and 10% inlet turbulence cases. All other experimental conditions were matched in the simulations including the temperature levels and flow rates.

To allow for reasonable computational times, all computations were performed using the RNG k-ε turbulence model with nonequilibrium wall functions whereby the near-wall region was resolved to y^+ values ranging between 30 and 60. Mesh insensitivity was confirmed through several grid adaptions based on viscous wall values, velocity gradients, and temperature gradients. Typical mesh sizes were composed of 1.8 million cells with 50% of the cells in and around the tip gap region. After adapting from a mesh of 1.7×10^6 to 2.2×10^6, the pitchwise-averaged effectiveness predictions on the tip were found to vary by only $\delta\eta=\pm0.007$ at a level of $\eta=0.40$. Typical computations required 1200 iterations for convergence.

Experimental Results for a Range of Blowing Ratios

Contour plots of local adiabatic effectiveness levels are given in this section to show the cooling trends for the two tip gaps for a range of cooling flow conditions. Adiabatic effectiveness levels of one note that the local wall temperature is at the coolant temperature while levels of zero refer to the hot gas temperature. To quantify the differences, data have been compared along various lines across the tip. These comparisons were made along different trajectory lines of the cooling jets (lines 1 and 2) and between the cooling jets (line 3) near the middle of the blade tip. Lines 1 and 2, referred to as line data, have been identified as locations having maximum effectiveness levels while line 3 is between two jet trajectories in the mid-chord region. A third comparison was made along the blade camber line as shown in the illustration of Fig. 8.

Comparisons for the Small Tip Gap. Figure 9 shows the measured adiabatic effectiveness levels along the blade tip for the small tip gap. Note that the exit of one hole location in the mid-chord region is indicated by a black dot along the pressure side. For proprietary reasons not all hole locations are disclosed. As will be discussed later in this text, the location of the cooling hole and the maximum effectiveness levels are not collocated. Although the results are only shown for one cooling hole, this result is representative of all cooling holes. For all cases shown in Fig. 9, the entire leading edge region is nearly completely cooled by the dirt purge holes. This leading edge area shows essentially no change as this entire region is saturated by coolant.

As the blowing ratio is increased for the small tip gap, Fig. 9 shows that there is relatively little increase in effectiveness or in coolant spreading. The effectiveness levels indicate a streaky nature, which is caused by the high momentum jets exiting the cooling holes. As will be discussed later in the text, while the effectiveness contours indicate little improvement in the global cooling characteristics along the blade tip with increased coolant flow, peak effectiveness levels along jet trajectories do increase with increased coolant flow.

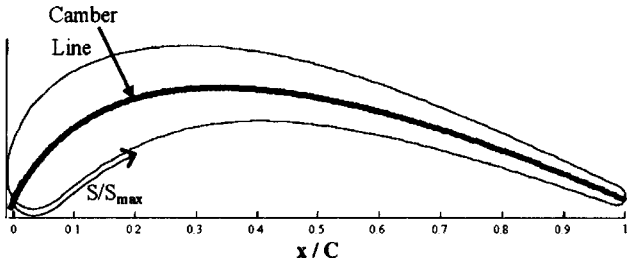

Fig. 8 Location and description of line data taken along blade tip

For the lowest coolant flow (0.47%) case, the effectiveness levels at the trailing edge show that the trailing edge is actually cooler at the lowest coolant flow. The higher effectiveness for the lower coolant flow is because the momentum flux ratios of these jets exiting the trailing edge holes are low, as indicated in Fig. 6 for the 0.47% cooling flow case, resulting in a cooler gap flow along the tip of the blade. This phenomena can be better understood by comparing the hole exit location to the jet trajectory. The upstream cooling hole jets are being swept downstream of the hole exit before entering the tip region. The reason for this is twofold: first, the cooling jets have a high enough momentum to overcome the driving pressure across the tip gap and, second, the jet injection angle forces the jets to follow the pressure side of the blade.

Computations were performed for the small tip gap for a total coolant flow of 0.58% to verify these flow patterns. Path lines exiting the holes are given in Fig. 10. In the mid-chord region, jets appear to be swept downstream before being carried over the tip. The predictions also indicate several jet trajectories where the coolant remains along the pressure side of the blade for most of the blade before entering into the downstream gap region. The holes in the leading edge have the highest blowing ratio, relative

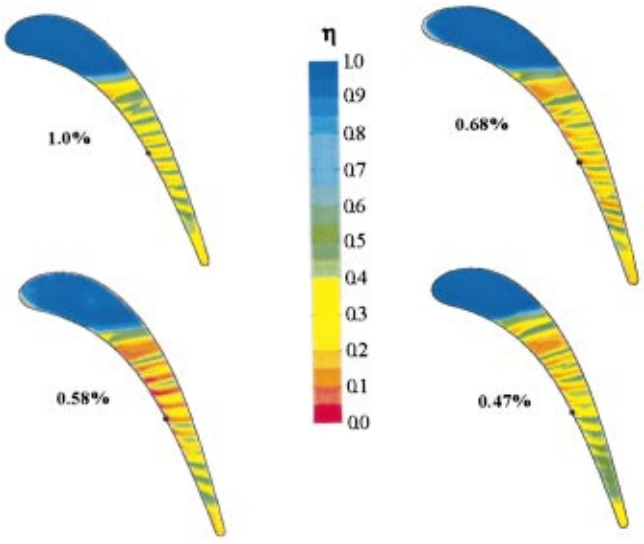

Fig. 9 Measured adiabatic effectiveness levels on the tip for the small tip gap

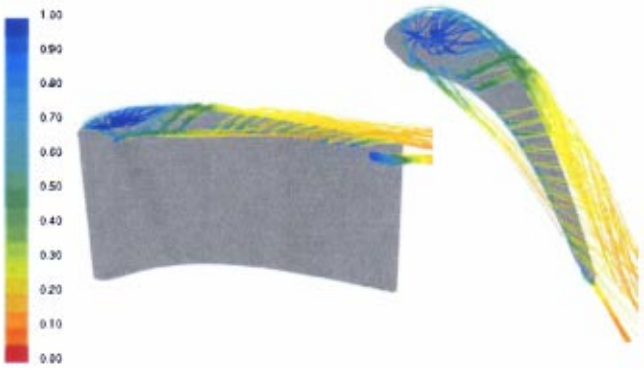

Fig. 10 Predicted path lines for the 0.58% coolant flow at the small tip gap

to the rest of the blade, so the prediction of jets following the blade pressure side rather than entering into the tip gap is expected.

Camber line comparisons for the small tip gap are shown in Fig. 11. Note that the distance x is shown as the abscissa of the graph illustrated in Fig. 8. For the same total coolant flow rate, the dirt purge flow dominates to $x/C=0.3-0.4$. For $x/C>0.6$, the effectiveness levels show relatively similar levels for both coolant flows with peaks and valleys ranging between 0.5 and 0.3. It is also interesting to note that the peak effectiveness levels for the two coolant flow conditions do not coincide. The peak for the 1% coolant flow occurs downstream of that for the 0.58% coolant flow. This is consistent with the jets having the higher blowing ratios being swept further downstream before entering the tip gap.

Comparisons for the Large Tip Gap. For the large tip gap results, shown in Fig. 12, the effectiveness levels are much lower than for the small tip gap (Fig. 9). The largest difference relative to coolant flow rates is near the dirt purge holes with better effectiveness levels at higher coolant flow levels. In particular, the largest improvement occurs for the 1% coolant flow condition with nearly perfect cooling of the entire leading edge.

In the mid-chord region, however, the results indicate a worse performance, as shown in Fig. 12, as the coolant flow is increased from of 0.47% to 1%. The reason for the worse performance at high blowing ratios is because the high momentum cooling jets are impinging upon the shroud and are not effective in cooling the blade tip, but are most likely effective in cooling the outer shroud. As the coolant levels are increased, the jet penetration above the blade tip severely reduces the cooling capabilities of the jet along

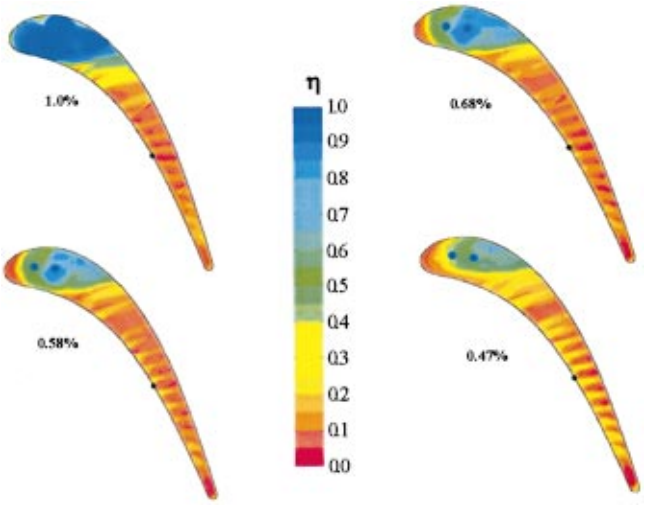

Fig. 12 Measured adiabatic effectiveness levels for the large tip gap

the tip. The hole locations given on these contour plots show the same results as seen with the small tip gap in that the peak effectiveness levels are located downstream of the injection location.

The camber line data for the large tip gap, shown in Fig. 13, indicate no cooling benefit beyond $x/C=0.4$ as the coolant is increased from 0.58% to 1%. In fact, the average appears to be similar for the two blowing cases with the exception that the 0.58% case has higher peaks and valleys than the 1% case. Similar to that of the small tip gap, the peaks in effectiveness are located further downstream for the 1% case relative to the 0.58% case.

Comparisons of Individual Holes. Figures 14(a)–(c) show line data of the effectiveness levels at blowing ratios of 0.58% and 1.0%. Note that the distance along the tip (L) was normalized with the maximum distance along the tip (L_{max}). Recall lines 1 and 2 are pathlines along the maximum effectiveness levels while line 3 is mid-way between pathlines of maximum effectiveness levels.

For each of the three positions shown in Figs. 14(a)–(c), the adiabatic effectiveness always increases with coolant flows for the small tip gap. These results indicate that the cooling potential is higher with higher coolant flows for the small tip gap. Even though the momentum flux ratios of the jets increase for increased coolant flow levels, the tip gap is small enough that coolant is forced to also be present along the blade tip.

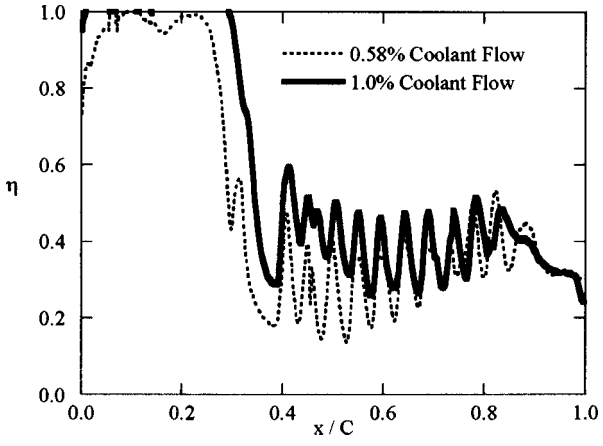

Fig. 11 Data taken along the camber line for the small tip gap at two blowing ratios

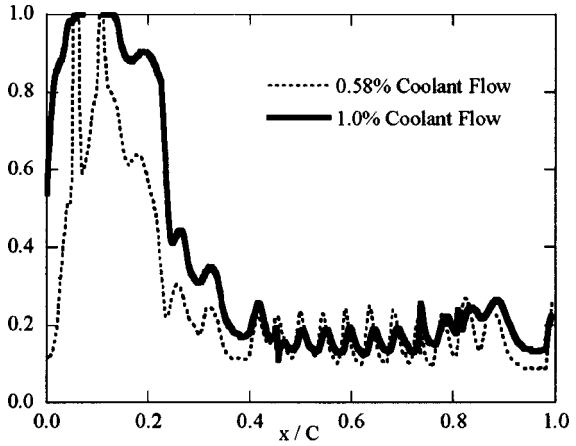

Fig. 13 Data taken along the camber line for the large tip gap

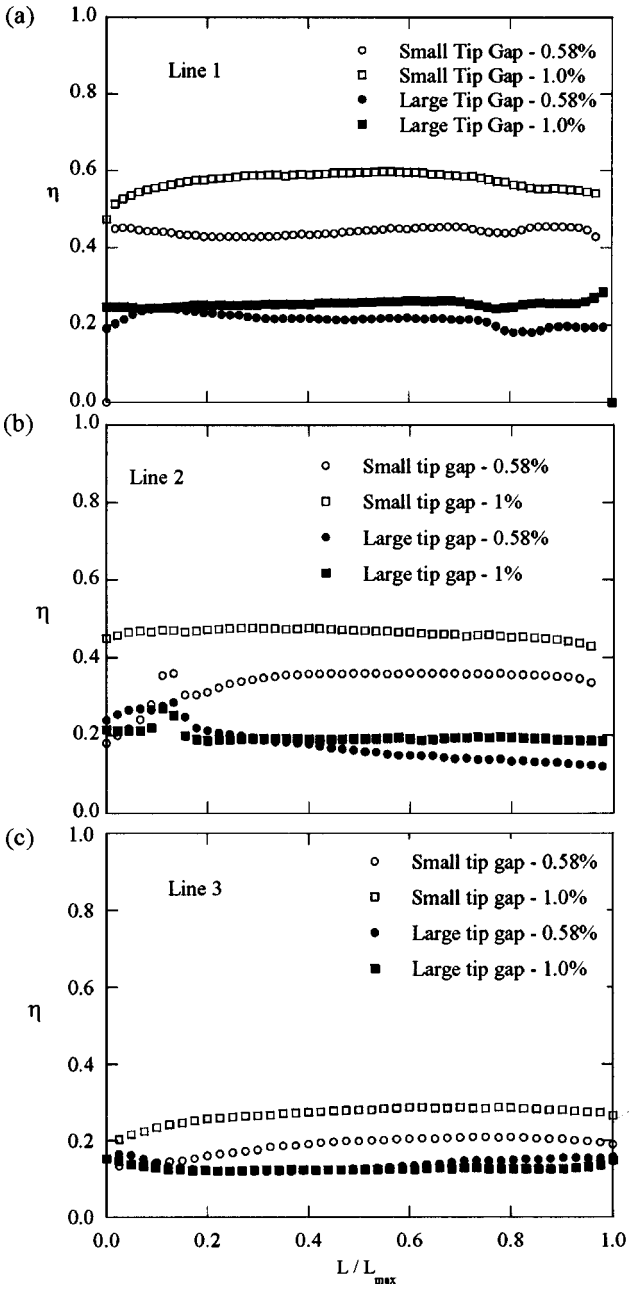

Fig. 14 (*a*)–(*c*) Line data for the different cases

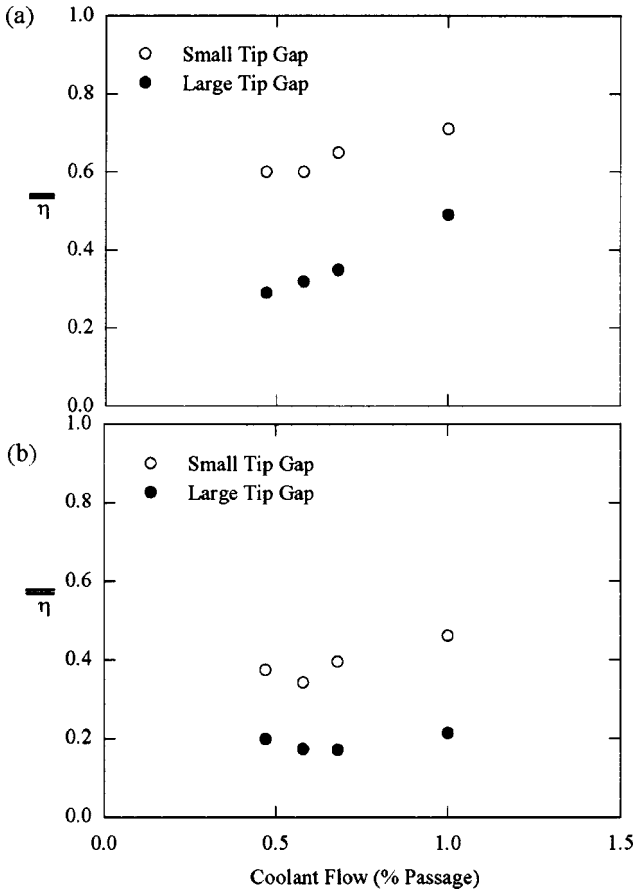

Fig. 15 Area-averages for (*a*) the entire blade tip and (*b*) the downstream 70% of blade

For the large tip gap, however, the same trend is not true as shown by Figs. 14(*a*)–(*c*). There are actually some segments of the blade where the effectiveness is higher with a lower blowing ratio, especially near the pressure side ($L/L_{max}<0.2$). The reason for this is because at the lower blowing ratios the coolant remains more attached to the blade tip. At higher blowing ratios, the coolant becomes separated from the blade tip and instead cools the outer shroud. Figure 14(*c*) shows data taken between two coolant trajectories. There is essentially no difference with increased blowing for the large tip gap, but a slight increase for the small tip gap because coolant fills the small gap region.

Area-averaged film effectiveness results were calculated using two different areas to make overall conclusions about the testing performed, as shown in Figs. 15(*a*) and 15(*b*). Figure 15(*a*) shows area-averaged effectiveness values for the entire tip while Fig. 15(*b*) shows area-averaged effectiveness values for the downstream 70% of the blade tip to better illustrate the performance of the cooling holes alone (without the effect of the dirt purge holes). Figure 15(*a*) indicates a relatively constant increase in area-averaged effectiveness with coolant flow increase for the large tip gap, but little increase in effectiveness for the small tip gap. The reason for this is because of the increase in effectiveness occurring near the dirt purge holes for the large tip gap. Recall that for the small tip gap, the coolant nearly saturated the leading edge region for all blowing ratios considered. Figure 15(*a*) also shows the overall trend that higher effectiveness levels occur for the smaller tip gap relative to the large tip gap.

Since much of the blade is dominated by dirt purge cooling, a better comparison on the effects of blowing from the pressure side holes can be made by considering the downstream 70% of the blade, as shown in Fig. 15(*b*). While the small tip gap shows a slight decrease with an increase in coolant flow for the first two conditions, beyond that there is an increase in effectiveness with increased coolant flow. For the large tip gap, the area averages indicate a slight decrease with increased coolant flow, which is then followed by only a slight increase in area-averaged effectiveness with values for the 0.47% and 1% coolant flows being at nearly the same level.

Leading Edge Blowing With no Dirt Purge Blowing. Because the dirt purge blowing overwhelms a large portion of the leading edge region, an additional test was conducted whereby coolant from only the film-cooling holes was exhausted in the leading edge (no dirt purge blowing). This case is also relevant from an engine operational standpoint whereby the dirt purge holes may be closed due to rubbing on the shroud. The coolant flow for this case was set to be the coolant exhaust that resulted for the 0.68% case subtracting out the dirt purge, tip flag, and back supply chamber cooling. This resulted in a total coolant flow of

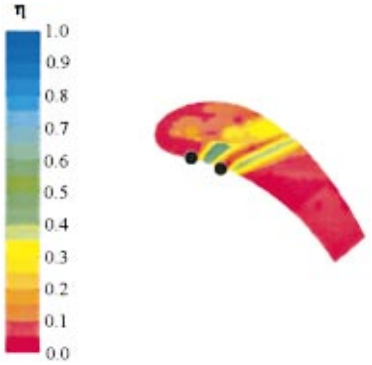

Fig. 16 Effectiveness contours with no dirt purge blowing with 0.07% coolant flow for the large tip gap

0.07% being injected from the first two holes. Figure 16 shows the measured results of this test for a small tip gap. Note that while the dirt purge holes were not flowing, the cavity was still present. The results for this test indicate that the coolant is being brought into the dirt purge cavity and then mixed with hot mainstream fluid before exiting at a much higher temperature. The hole locations indicate that in the leading edge region, without dirt purge blowing, the coolant is swept significantly further downstream of their respective hole exits.

Conclusions

The conclusions reached from these tests indicate that the performance of cooling holes placed along the pressure side tip was better for a small tip gap than for a large tip gap. Disregarding the area cooled by the dirt purge holes, for a small tip gap the cooling holes provided relatively good coverage. For all of the cases considered, the cooling pattern was quite streaky in nature, indicating very little spreading of the jets.

As the blowing ratio was increased for the small tip gap, there was an increase in the local effectiveness levels resulting in higher maxima and minima of effectiveness along the middle of the blade. The small tip gap results also indicated that the coolant was swept further downstream of the hole along the pressure side of the blade prior to entering the tip gap for higher coolant flows, particularly those holes in the leading edge region. In fact, computational predictions and measured effectiveness levels for the low coolant flows indicated that the jets exited into the pressure side passage following the pressure side of the blade until the trailing edge of the blade at which point the coolant entered the tip gap. Although the local momentum flux ratio of the jets increased with increased coolant flow, the coolant still appeared to cool the blade tip, which was different from that of the large tip gap.

For the large tip gap, the data indicated that the adiabatic effectiveness levels decreased, or remained relatively constant, as the coolant flow was increased. As the coolant flow was increased the jets most likely impacted and cooled the outer shroud of the large tip gap rather than the blade tip. The distance between the blade tip and outer shroud were far enough apart that there was little cooling benefit to the blade. These results indicate the importance not only from an aerodynamic loss standpoint but also a thermal standpoint of keeping the tip gap small.

Acknowledgments

The authors gratefully acknowledge United Technologies–Pratt and Whitney for their support of this work.

Nomenclature

C = true chord of blade
C_d = discharge coefficient, $C_d = \dot{m}/(\rho A\sqrt{(2/\rho)(P_{0,c}-p_e)})$
C_p = pressure coefficient, $C_p = (p-p_{in})/(\rho U_{in}^2/2)$
D = dirt purge hole diameter
D_h = hydraulic diameter, set as twice the gap height
h, H = small and large gap distances
L = distance along the path line across the tip
M = mass flux ratio
P_o, p = total and static pressures
$\mathrm{Re_{in}}$ = Reynolds number defined as $\mathrm{Re_{in}} = CU_{in}/\nu$
S = distance along blade pressure side from stagnation
T = temperature
U = measured air velocity
x = distance along the blade chord

Greek

Δ = denotes a differential
η = adiabatic effectiveness, $\eta = (T_{\mathrm{in}}-T_{\mathrm{aw}})/(T_{\mathrm{in}}-T_c)$
ρ = density
ν = kinematic viscosity

Subscripts

aw = adiabatic wall
b = blade
c = coolant conditions
dyn = dynamic
in, e = value at 1C upstream of blade, exit
max = denotes maximum value

References

[1] Christophel, J., Thole, K. A., and Cunha, F., 2005, "Cooling the Tip of a Turbine Blade Using Pressure Side Holes—Part II: Heat Transfer Measurements," ASME J. Turbomach. **127**, pp. 278–286.
[2] Bunker, R. S., 2000, "A Review of Turbine Blade Tip Heat Transfer," Turbine 2000 Symposium on Heat Transfer in Gas Turbine Systems, Cesme, Turkey.
[3] Kim, Y. W., and Metzger, D. E., 1995, "Heat Transfer and Effectiveness on Film Cooled Turbine Blade Tip Models," ASME J. Turbomach., **117**, pp. 12–21.
[4] Kim, Y. W., Downs, J. P., Soechting, F. O., Abdel-Messeh, W., Steuber, G., and Tanrikut, S., 1995, "A Summary of the Cooled Turbine Blade Tip Heat Transfer and Film Effectiveness Investigations Performed by Dr. D. E. Metzger," ASME J. Turbomach., **117**, pp. 1–11.
[5] Kwak, J. S., and Han, J. C., 2002, "Heat Transfer Coefficient and Film-Cooling Effectiveness on a Gas Turbine Blade Tip," GT2002-30194.
[6] Kwak, J. S., and Han, J. C., 2002, "Heat Transfer Coefficient and Film-Cooling Effectiveness on the Squealer Tip of a Gas Turbine Blade," GT2002-30555.
[7] Acharya, S., Yang, H., Ekkad, S. V., Prakash, C., and Bunker, R., 2002, "Numerical Simulation of Film Cooling Holes on the Tip of a Gas Turbine Blade," GT-2002-30553.
[8] Hohlfeld, E. M., Christophel, J. R., Couch, E. L., and Thole, K. A., 2003, "Predictions of Cooling From Dirt Purge Holes Along the Tip of a Turbine Blade," GT2003-38251.
[9] Srinivasan, V., and Goldstein, R. J., 2003, "Effect of Endwall Motion on Blade Tip Heat Transfer," ASME J. Turbomach., **125**, pp. 267–273.
[10] Ameri, A. A., 2001, "Heat Transfer and Flow on the Blade Tip of a Gas Turbine Equipped With a Mean-Camberline Strip," 2001-GT-0156.
[11] Moffat, R. J., 1988, "Describing the Uncertainties in Experimental Results," Exp. Therm. Fluid Sci., **1**, pp. 3–17.
[12] Fluent Inc., Fluent User's Guide, Version 6.0, 2002 (Fluent Inc., New Hampshire).